



# Parallel disulfido bridges in bi- and poly-nuclear transition metal compounds: Bonding flexibility induced by redox chemistry

Carlo Mealli<sup>a,\*</sup>, Andrea Ienco<sup>a</sup>, Abdelatif Messaoudi<sup>a</sup>, Anne Poduska<sup>b</sup>, Roald Hoffmann<sup>b</sup>

<sup>a</sup>Istituto di Chimica dei Composti Organometallici, ICCOM-CNR, Via Madonna del Piano 10, 50019 Sesto Fiorentino, Firenze, Italy

<sup>b</sup>Department of Chemistry and Chemical Biology, Baker Laboratory, Cornell University, Ithaca, NY 14853-1301, USA

## ARTICLE INFO

### Article history:

Received 22 February 2008

Accepted 13 March 2008

Available online 18 March 2008

Dedicated to Professor Dante Gatteschi.

### Keywords:

Disulfide bridges

Coupling of sulfides

S<sub>4</sub> rings

S<sub>2</sub><sup>2-</sup>/S<sub>4</sub><sup>2-</sup> dichotomy

DFT calculations

Qualitative MO analysis

## ABSTRACT

We recently studied an elongated S<sub>4</sub><sup>2-</sup> rectangle bridging transition metals such as Ir, Rh, Cu, or Fe and found that its formation is related to the oxidation of parallel S<sub>2</sub><sup>2-</sup> molecules. The removal of two electrons can occur either externally or by an internal metal–ligand redox process that implies depopulation of the high-lying S<sub>4</sub> σ\* MO and population of a lower metal level. Thus, the interaction may be described as metal back-donation. However, sufficiently electropositive metals can more easily reach higher oxidation states and this reverses the direction of the two-electron interaction. In such a case, the system may be viewed as formed by two uncoupled disulfides donating an additional electron pair to the metals. In this paper, we analyze the aspects of the 2S<sub>2</sub><sup>2-</sup>/S<sub>4</sub><sup>2-</sup> dichotomy through DFT calculations and qualitative MO analysis of the known bimetallic MS<sub>4</sub>M cores having either triple-decker (TD) or chair-type structures. We correlate the extent of the disulfide coupling with the nature (electronegativity) of the terminal metal fragments (the metals range from Group IV to X) beside their electron configuration. We find that the formation of an S<sub>4</sub><sup>2-</sup> unit is favored by metals which cannot stabilize high oxidation states (e.g. Fe(IV) or Cu(III)), whereas the two S<sub>2</sub><sup>2-</sup> units remain substantially uncoupled with early transition metal in high oxidation states (e.g. Ti(IV)).

© 2008 Elsevier B.V. All rights reserved.

## 1. Introduction

### 1.1. A precedent for formation of S<sub>4</sub><sup>2-</sup>

In a recent paper [1], we pointed out the unusual capability of two metal-coordinated S<sub>2</sub><sup>2-</sup> units to couple together and form a S<sub>4</sub><sup>2-</sup> ring upon two-electron oxidation. The latter process can be promoted either by an external oxidizing agent or an inner redox process in which the metal atoms undergo a two-electron reduction. An unequivocal example of coupled disulfides is provided by the chemical oxidation of the dinuclear species Cp\*Ir(μ-CH<sub>2</sub>)<sub>2</sub>(μ-S<sub>2</sub>)IrCp\* and the formation of the tetranuclear compound [(Cp\*<sub>2</sub>Ir<sub>2</sub>(μ-CH<sub>2</sub>)<sub>2</sub>)<sub>2</sub>(μ-S<sub>4</sub>)]<sup>2+</sup> (see **1** in Chart 1a [2]). In the Ir<sub>2</sub>S<sub>2</sub> precursor of **1**, S<sub>2</sub><sup>2-</sup> dative coordination to the M<sub>2</sub> unit occurs with two filled S p<sub>z</sub> orbitals (see Chart 1b), while the π and π\* combinations of the p<sub>y</sub> orbitals (to be discussed shortly) play a fundamental role for the dimerization of the M<sub>2</sub>S<sub>2</sub> units. The resulting S<sub>4</sub><sup>2-</sup> ring is an elongated rectangle with long sides of 2.894(3) Å and short sides of 2.049(3) Å, that are even shorter than in the S<sub>2</sub><sup>2-</sup> unit of the binuclear precursor (2.126(10) Å). This is likely the effect of the reduced local repulsion within the S<sub>2</sub><sup>2-</sup> ligands following the system's oxidation.

The replacement of iridium with rhodium [3] also leads to a tetranuclear cluster with a chair-like structure (**2**), but there are several differences. One, the redox process is not equally straightforward as that leading to **1**. Two, the S<sub>4</sub><sup>2-</sup> rectangle has a different orientation with respect to the two binuclear units, the long S··S vectors being parallel – not perpendicular – to the Rh–Rh bonds (see Chart 1a). The theoretical underpinnings of the reactivity leading to either S<sub>4</sub><sup>2-</sup> orientation (as found in **1** or **2**) will be presented elsewhere [4].

### 1.2. The orbitals of two S<sub>2</sub><sup>2-</sup> units in anticipation of forming S<sub>4</sub><sup>2-</sup>

DFT and qualitative MO analysis of **1** and **2** have provided a reasonable explanation for the observed rectangular deformation of the S<sub>4</sub><sup>2-</sup> unit [1]. In order to summarize the arguments, Fig. 1 shows all of the significant σ (Fig. 1a) and π combinations (Fig. 1b and c) of the two S<sub>2</sub><sup>2-</sup> units (labels inside the rectangle) that interact, via loss of two electrons, to form a S<sub>4</sub><sup>2-</sup> ring. As indicated by the labels outside the rectangle, along the pathway the π<sub>y</sub> combinations form the σ and σ\* combinations of the new S–S linkages. The combinations perpendicular to the S<sub>4</sub> plane (Fig. 1c) are all populated and used to make dative σ bonds to the metal atoms in **1** and **2** as well as in their precursors (Chart 1b). Incidentally, recall that the d<sup>7</sup>–d<sup>7</sup> metal configuration in all cases implies a direct M–M bond (as confirmed by the short observed distance), which is

\* Corresponding author. Tel.: +39 0555225884; fax: +39 0555225203.  
E-mail address: carlo.mealli@iccom.cnr.it (C. Mealli).

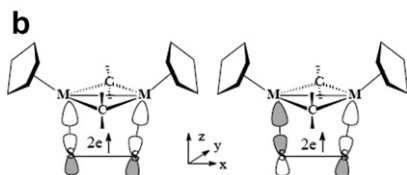
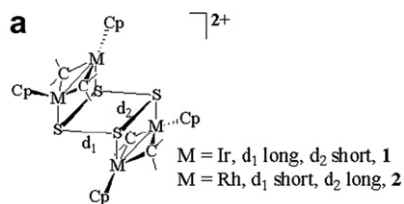
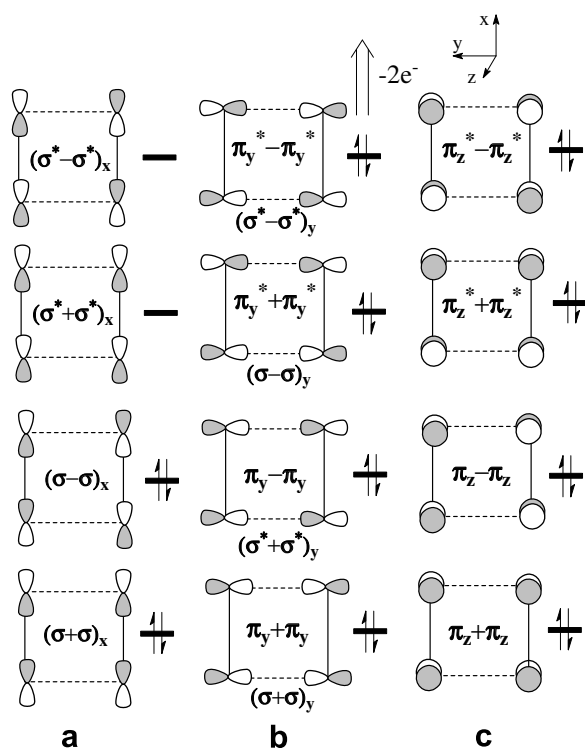


Chart 1.



**Fig. 1.** Combinations of all the sulfur p orbitals in two parallel  $S_2^{2-}$  units. The + and – signs refer to the in- and out-of-phase combinations along the y-axis. On reducing the separation between the two  $S_2^{2-}$  units, the  $\pi_y^* - \pi_y^*$  level is the first candidate to lose its electrons, as highlighted by the arrow.

unaffected by the  $2e^-$  oxidation process mainly involving the S atoms.

Along the x-axis (which runs parallel to the Ir–Ir bonds in **1**), the four combinations of the S  $p_x$  orbitals (Fig. 1a) are populated by four electrons, which is consistent with the presence of two single S–S bonds. In contrast, all of the  $p_y$  combinations in Fig. 1b are initially populated in the two  $S_2^{2-}$  units and represent the equivalent of four S lone pairs. Coupling of the disulfides along the y-axis forces pairwise separations of the different  $p_y$  combinations in view of the acquired  $\sigma$  and  $\sigma^*$  character relative to the new S–S linkages. The coupling process is likely triggered by the early depopulation of the high-lying level  $\pi_y^* - \pi_y^*$ , since we have computationally found that the monocationic derivative of dinuclear precursors of **1** and **2** are stable as radical species [1].

The lower  $\pi_y - \pi_y$  combination also acquires antibonding character  $(\sigma^* + \sigma^*)_y$  on coupling and may eventually lose its electrons.

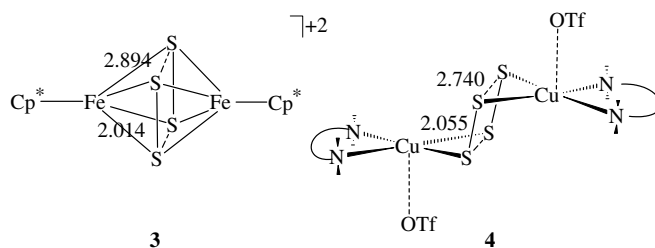


Chart 2.

Computationally, we have proved the hypothetical tetracation  $[(Cp^*_2Ir_2(\mu-CH_2)_2)_2(\mu-S_4)]^{4+}$  with an uncharged  $S_4$  bridge is a minimum [1]. In practice, however, the second two-electron oxidation may be difficult. In fact, the  $\pi_y^* + \pi_y^*$  level, which stabilizes as a  $(\sigma - \sigma)_y$  bonding combination, starts in the calculations at an energy higher than that of the destabilizing  $\pi_y - \pi_y$  level. The removal of two electrons from the latter is possible only after the inter-level crossing has occurred, otherwise the 2+2 cycloaddition is symmetry forbidden. However, given the stability of **1** with a rather large separation between the two  $S_2$  units,  $(\sigma^* + \sigma^*)_y$  hardly attains an energy sufficiently high for its straightforward oxidation. In conclusion, the bridging  $S_4$  unit in **1** (but also in **2**) is preferentially stabilized as a  $S_4^{2-}$  ring with pairs of S–S bonds having order 1 and 0.5, respectively.

### 1.3. Where else might $S_4^{2-}$ be?

The chemical, structural and computational evidence for the rare rectangular  $S_4^{2-}$  ring in **1** and **2** has prompted us to inquire whether such a unit may exist in other chemical compounds. Some such molecules might have passed unrecognized because of their long S–S bonds. In fact, in surveying the literature, a common assumption appears that S–S interactions at distances  $\geq 2.7$  Å should be nonbonding. We found in the Cambridge Structural Database (CSD)<sup>1</sup> at least two other candidates (Chart 2) that could – and do, by our reasoning – contain a  $S_4^{2-}$  ring [1]. These are the triple-decker (TD) compound  $[Cp^*Fe(\mu-S_2)_2FeCp^*]X_2$ , **3** ( $X = I^-$ , [5]  $X = PF_6^-$  [6]), and the chair species  $[L_2Cu_2(\mu-S_2)_2](OTf)_2$ , **4** ( $L_2 = Me_2NCH_2CH_2NMe_2$ ; OTf = weakly coordinated triflate anion [7]). Our search has also given us a few candidates where a direct coupling of the disulfide bridges is more questionable: in binuclear systems with TD or chair-like  $MS_4M$  cores. The TD compounds have already received some theoretical attention [9], but here we provide new computational results for chair systems containing  $Co_2$ , [10]  $Ru_2$ , [11,12]  $Mn_2$ , [13] and  $Ti_2$  [14] metals (all retrieved from the CSD,<sup>1</sup> in which the separation of the two parallel  $S_2$  units is  $\geq 3.1$  Å).

In our discussion, we will first outline our arguments for a  $S_4^{2-}$  ring in **3** and **4**, and then extend this to other compounds, paying attention to the nature of the transition metal and how it plays a role in preventing the coupling of the two  $S_2^{2-}$  parallel bridges. We also show, however, that even at long S–S distances, there may be a small degree of S–S coupling present.

## 2. Discussion

### 2.1. Binuclear systems with an $S_4^{2-}$ bridge

The MO arguments developed for the compounds **3** and **4** [1] are necessary for a general description of the  $2S_2^{2-}/S_4^{2-}$  dichotomy in  $M_2S_4$  frameworks. The former is a triple-decker (TD) where two

<sup>1</sup> Cambridge Structural Database System, Cambridge Crystallographic data Centre, 12 Union Road, Cambridge CB2 1EZ, UK.

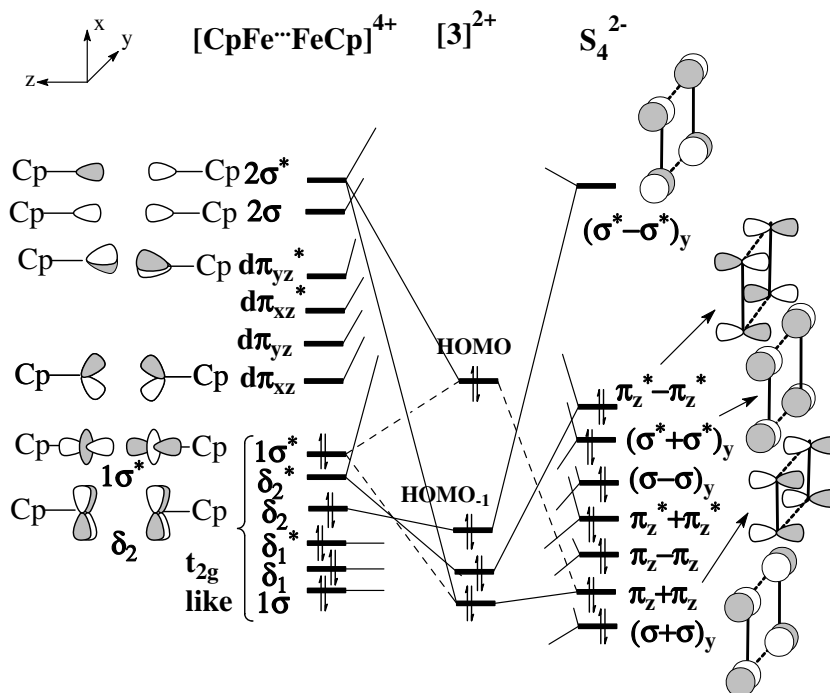


**Fig. 2.** Interaction diagram for  $[\text{CpFe}(\mu\text{-S}_4)\text{FeCp}]^{2+}$ ,  $[\mathbf{3}]^{2+}$ . Eight positive bonding interactions are formed between the following FMO pairs: (1)  $2\sigma/(\sigma+\sigma)_y$ ; (2)  $2\sigma^*/\pi_z+\pi_z$ ; (3)  $d\pi_{yz}/\pi_z-\pi_z$ ; (4)  $d\pi_{xz}/\pi_z^++\pi_z^+$ ; (5)  $d\pi_{xz}/(\sigma-\sigma)_y$ ; (6)  $d\pi_{yz}/(\sigma^++\sigma^+)_y$ ; (7)  $\delta_2^*/\pi_z^--\pi_z^+$ ; (8)  $(\sigma^--\sigma^*)_y/\delta_2$ .

$\text{Cp}^*\text{Fe}$  fragments bicap the  $\text{S}_4$  rectangle with sides of 2.014 and 2.894 Å, respectively. The dicopper complex **4** has instead a chair-like conformation, where the metals coordinate the long S–S sides, similar to **2**. Their illustration requires continuous reference to the  $\text{S}_4$  orbitals in Fig. 1.

Fig. 2 presents an interaction diagram for a model of the TD dication **3**. The known MOs of two  $\text{CpFe}$  fragments [18] are reported at the left side and consist of higher combinations of  $\sigma$  and  $d_\pi$  hybrids (two orthogonal sets) plus two sets of lower  $t_{2g}$ -like levels. On the right side, there are eight of the twelve  $\text{S}_4$  levels presented in Fig. 1.

We will not consider the other four orbitals of Fig. 1a, as they are low-lying and involved in the short S–S bonds. The existence of eight Fe–S connectivities is confirmed by the positive overlap populations (OP) between eight different FMO pairs. These bonds include two  $t_{2g}$  metal combinations besides those of the six higher  $\sigma$  and  $d_\pi$  metal hybrids. The  $\text{S}_4$  grouping participates with the four combinations of the upright  $p_z$  orbitals and the in-plane  $p_y$  ones. For convenience, the latter four are expressed by the  $\sigma/\sigma^*$  notation relative to the new potential S–S bonds rather than the  $\pi_y/\pi_y^*$  one (both labels are indicated in Fig. 1).

The important point to be made is that seven interactions are dative toward the metals, including the  $\delta_2^*$  combination of  $t_{2g}$  orbitals with  $\delta$  symmetry, which may be considered empty for the  $\text{Fe(III)}\text{--Fe(III)}$  configuration. Also, the corresponding in-phase combination  $\delta_2$  is involved, but its interaction with  $(\sigma^--\sigma^*)_y$  should be regarded as a metal back-donation in view of the high energy of the  $\text{S}_4$  level that combines  $\sigma^*$  and  $\pi^*$  antibonding character. In order to invert the electron flow in the latter (i.e., a vacant  $\delta_2$  level and  $\text{Fe(IV)}$  metals), the separation between the two  $\text{S}_2$  units should be significantly larger than the observed 2.894 Å value. For us, this is the first example indicating how the electronegativity of a given metal prevents the attainment of a high oxidation state (at least in the absence of very electronegative ligands), hence the coupling between two  $\text{S}_2^{2-}$  units.

Since the separation between the two  $\text{S}_2$  diatomics in the dicopper chair complex **4** is about 0.15 Å shorter than in **3**, the presence

of a  $\text{S}_4^{2-}$  unit is even more likely here. Again, in presence of sulfide ligands, the metals have some difficulty in attaining a higher oxidation state such as  $\text{Cu(III)}$ , which is not very common (at least in the absence of very electronegative ligands such as oxygen donors). The overall MO picture compares with that in Fig. 2. By neglecting the weak axial interactions with the triflate anions, the two metals have approximate square planar coordination and the bonding with  $\text{S}_4$  involves the  $\sigma$  and  $d_\pi$  hybrids of the classic  $\text{L}_2\text{M}$  fragments. By assuming  $d^9\text{--}d^9$  configuration, two electrons must populate one of the four levels formed by the latter, which are not all acceptors. Indeed, there are three  $\text{S}_4 \rightarrow \text{Cu}_2$  dative interactions (i.e.,  $\pi_z+\pi_z \rightarrow \sigma^*$ ;  $\pi_z^++\pi_z^+ \rightarrow \sigma$  and  $\pi_z^--\pi_z^- \rightarrow d\pi$ ) and one  $\text{Cu}_2 \rightarrow \text{S}_4$  back-donation. Chart 3 highlights the behavior of the populated  $d_\pi^*$  metal level, which is destabilized by the lower  $\text{S}_4$   $\pi_z-\pi_z$  combination but redirects a part of its electron density toward the higher  $\text{S}_4$   $(\sigma^--\sigma^*)_y$  level. Since the latter is computed to be populated as little as 9%, it seems legitimate to invoke the existence of a  $\text{S}_4^{2-}$  ring with two S–S linkages  $\sim 0.5$  bond order each. As mentioned, the bonding

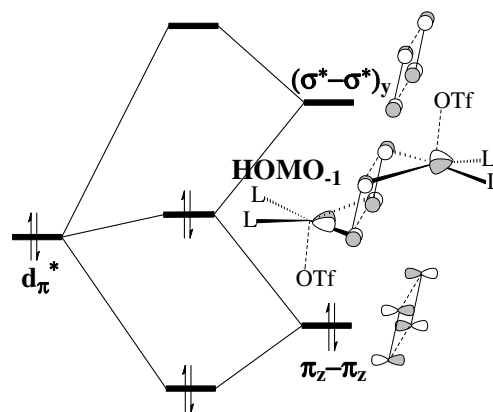


**Chart 3.**

**Table 1**  
A selection of the analyzed complexes  $L_nMS_4ML_n$  complexes with either triple-decker (TD) or chair-like conformation

Compound	Type	S–S $d_{\text{short}}$	S–S $d_{\text{large}}$	M–M dist.	Oxid. state	CSD refcode	Ref.
$[\text{Cp}^* \text{Fe}(\mu\text{-S}_4)\text{FeCp}^*]^{2+}$ , <b>3</b> <sup>a</sup>	TD	2.01 2.02	2.89 3.02	2.87 2.88	Fe(III)	GEMSAS	[5,6]
$[\text{Cp}^* \text{Re}(\mu\text{-S}_2)_2 \text{ReCp}^*]^{2+}$ , <b>5</b> <sup>b</sup>	TD	2.23	3.24	2.61	Re(IV)	RITNOX	[15]
$[\text{Cp}^* \text{Mo}(\mu\text{-S}_2)(\mu\text{-S})_2 \text{MoCp}^*]$ , <b>6</b>	TD	2.09 <sup>c</sup>	3.97	2.60	Mo(IV)	BOBVOD	[16]
$[\text{Cp}^* \text{Cr}(\mu\text{-S}_2)(\mu\text{-S})_2 \text{CrCp}^*]$ , <b>7</b>	TD	2.11 <sup>c</sup>	3.85	2.46	Cr(IV)	SAHMET	[17]
$(\text{OTf})\text{L}_2\text{Cu}(\mu\text{-S}_4)\text{CuL}_2(\text{OTf})$ , <b>4</b> <sup>d</sup>	chair	1.95 1.98	2.74 2.81	4.56 4.78	Cu(II)	CEDCOE	[7]
$[\text{L}_4\text{Co}(\mu\text{-S}_2)_2 \text{CoL}_4]^{2+}$ , <b>8</b> <sup>e, f</sup>	chair	2.01 2.06	3.13 3.23	4.75 4.82	Co(III)	GUNRIQ	[10]
$\text{Cp}'(\text{PPh}_3)\text{Ru}(\mu\text{-S}_2)_2 \text{Ru}(\text{PPh}_3)\text{Cp}'$ , <b>9</b> <sup>g</sup>	chair	2.05 2.07	3.53 3.59	4.29 4.34	Ru(III)	FORCAQ	[11]
$\text{Cp}(\text{P}(\text{OMe})_3)\text{Ru}(\mu\text{-S}_2)_2 \text{Ru}(\text{P}(\text{OMe})_3)\text{Cp}$ , <b>10</b>	chair	2.04	3.54	4.27	Ru(III)	SOMYAU	[12]
$\text{Cp}(\text{NO})\text{Mn}(\mu\text{-S}_2)_2 \text{Mn}(\text{NO})\text{Cp}$ , <b>11</b>	chair	2.02 2.03	3.46 3.54	4.38 4.44	Mn(II)	REGTED	[13]
$(\text{Cp}'')_2\text{Ti}(\mu\text{-S}_2)_2 \text{Ti}(\text{Cp}'')_2$ , <b>12</b> <sup>h</sup>	chair	2.06 <sup>i</sup> 2.11	3.50 <sup>i</sup> 3.57	4.77 <sup>i</sup> 4.77	Ti(IV)	FEHTOB	[14]

The geometric parameters in italics refer to the DFT optimized models. All reported distances are in Å.

<sup>a</sup>  $\text{Cp}^* = [\text{C}_5(\text{CH}_3)_5]^-$ . The complex dication is present also in another structure with refcode GALVUX.

<sup>b</sup>  $\text{Cp}^* = \text{ethyl-tetramethyl-cyclopentadienyl}$ .

<sup>c</sup> The distance relative to the uncoupled sulfido anions is 3.10 and 3.02 Å for **6** and **7**, respectively.

<sup>d</sup>  $\text{L}_2 = \text{Me}_2\text{NCH}_2\text{CH}_2\text{NMe}_2$ ; OTf = triflate anion.

<sup>e</sup>  $\text{L}_4 = 1,4,8,12\text{-tetra-azacyclopentadecane}$  (cyclam).

<sup>f</sup> Two practically equal structures of the dication have been reported with different counterions, i.e.,  $\text{ClO}_4^-$  (GUNRIQ) and  $\text{BPh}_4^-$  (GUNROW).

<sup>g</sup>  $\text{Cp}' = \text{methyl-cyclopentadienyl}$ .

<sup>h</sup>  $\text{Cp}'' = \text{isopropyl-cyclopentadienyl}$ .

<sup>i</sup> Average values for two independent molecules.

interaction between the two  $\text{S}_2$  components in **4** has also received recent experimental support [8].

As another consideration, the  $d^9$  configuration proposed for each metal could raise a problem of spin-pairing between two largely separated metal atoms. The MO picture above clearly indicates that the  $\text{S}_4^{2-}$  bridge has an important role in forcing spin-pairing in the  $d_{\pi}^*$  level (this allows the back-donation) and consequently the system's stability can be related to a strong,  $\text{S}_4^{2-}$  induced, anti-ferromagnetic interaction.

## 2.2. Bimetallic systems with separated $\text{S}_2^{2-}$ bridges

At this point, we address other known cases in which no *trans*-annular interaction is predictable between the disulfide bridges of the  $\text{M}_2\text{S}_4$  core (either of the TD or chair-types). The examples are not particularly numerous and in general the large S–S separations are  $>3.1$  Å. Table 1 presents the known structures of TD and chair compounds with a  $\text{M}_2\text{S}_4$  core (irrespective of the disulfide coupling) together with some selected geometric parameters. Please consider that only the TD species with terminal Cp ligands have been addressed, but there are several additional examples of other comparable species with discrete terminal ligands in place of the Cp rings that we have not considered here.

Concerning the TD compounds, we have already indicated [1] that the  $\text{Re}_2$  species **5** [15] has in total two less electrons than the Fe system **3**. Thus with respect to the diagram in Fig. 2, the frontier M–M  $\sigma^*$  level is vacant, suggesting the presence of a direct Re–Re bond. This is corroborated by the short Re–Re distance of 2.61 Å. By looking at the nature of the HOMO in Fig. 2, we see that the situation is slightly complicated. The destabilizing interaction between the filled levels  $1\sigma^*$  and  $\pi_z + \pi_z$  becomes  $\text{M}_2\text{-S}_4$  bonding if the HOMO is depopulated and, in a sense, the M–M  $1\sigma^*$  level replaces  $2\sigma^*$  as the acceptor of the electron density in  $\pi_z + \pi_z$ . Now, since  $1\sigma^*$  and  $2\sigma^*$  are both involved in bonding with the sulfur bridges, a M–M bond can be considered only by the simultaneous population and depopulation of the  $1\sigma$  and  $2\sigma^*$  levels, respectively (obviously there is also some remixing of the metal  $\sigma$  components).

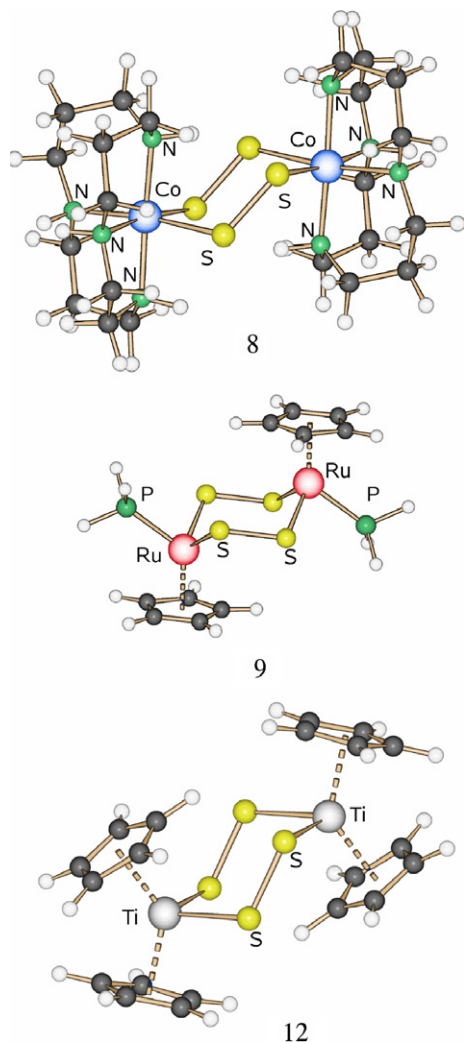
Importantly, the flattening of the TD structure upon Re–Re bond formation causes further stretching of the  $\text{S}_4$  rectangle. At the long

experimental S–S separation of 3.24 Å, the gap between the interacting levels  $\delta_2$  and  $(\sigma^* - \sigma^*)_y$  is reduced with respect to that in **3** (see Fig. 2) but we calculate that  $(\sigma^* - \sigma^*)_y$  still lies about 0.5 eV above  $\delta_2$  and is populated 40% (it was only 21% in **3**). Certainly, the  $\text{Re}_2$  system **5** favors, much more than **4**, uncoupled disulfide bridges. But a residual interaction between the latter may not be completely ruled out.

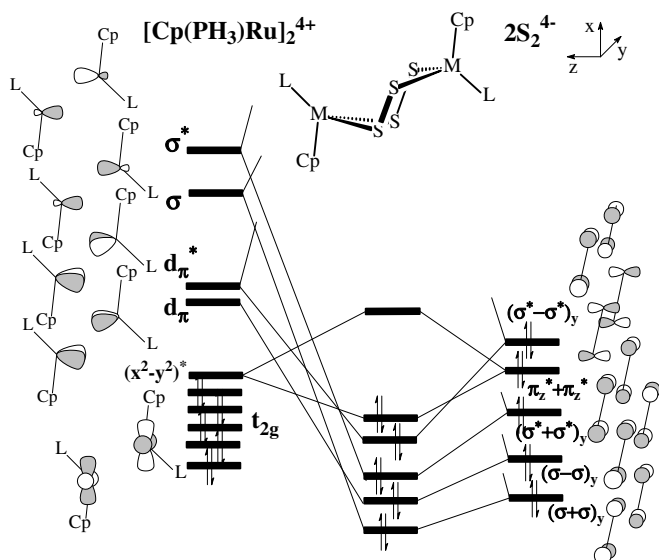
The TD  $\text{Mo}_2$  and  $\text{Cr}_2$  compounds **6** and **7** are isoelectronic with **5**. Here, not only there is practically no coupling of the disulfide bridges, but one of them is further split into two  $2\text{S}^{2-}$  anions, so that the metal configuration is  $d^2\text{-}d^2$ . In our previous analysis [1], we proposed that a symmetry forbidden HOMO–LUMO crossing along the coupling/uncoupling pathway of two sulfido anions prevents the interconversion of potential isomers which correspond to the structures of the isoelectronic complexes **5** and **6** (or **7**).

Fig. 3 presents the three-dimensional pictures of the chair-like compounds **8**, **9**, and **12** that have been also optimized with DFT calculations. In general, the computed parameters can be considered satisfactory, as they confirm the experimental geometries with the large separation between the two  $\text{S}_2^{2-}$  units. Notice in particular that in the  $\text{Co}_2$  complex **8**, the separation of 3.13 Å is about 0.23 Å larger than in compounds **1** and **3** (2.89 Å), but it is also 0.4 Å shorter than in **9–12** (3.47–3.54 Å).

Qualitative MO analysis helps to understand the electronic effects due to the nature of the metal atoms and the somewhat different S–S separations in the series **8–12**. Similarities within the series **8–11** are expected because the butterfly  $\text{L}_4\text{M}$  and the  $\text{CpLM}$  fragments are in principle *islobal* [19]. The frontier orbitals consist of pairs of  $\sigma$  and  $d_{\pi}$  empty metal hybrids, which are potential acceptors of four dative bonds from the bridging sulfur ions. Compared with the  $\text{Cu}_2\text{S}_4$  complex **4**, whose  $\text{L}_2\text{M}$  fragments (with exclusion of the triflate) are *islobal* with the  $\text{L}_4\text{M}$  and the  $\text{CpLM}$  ones, a difference arises from the population/vacancy assigned to the  $d_{\pi}^*$  level. For instance, there could be a close analogy between **4** and **8** by assuming that the latter is formed by  $\text{Co(II)}$  rather than  $\text{Co(III)}$  ions. Since cobalt is more electropositive than copper, its  $d_{\pi}^*$  level must lie relatively higher in energy while the larger separation between the  $\text{S}_2$  units keeps lower the  $\text{S}_4$   $(\sigma^* - \sigma^*)_y$  level. Even-



**Fig. 3.** Structures of the models  $[(\text{cyclam})\text{Co}(\mu\text{-S}_2)_2\text{Co}(\text{cyclam})]^{2+}$ ,  $\text{Cp}(\text{PH}_3)\text{Ru}(\mu\text{-S}_2)_2\text{Ru}(\text{PH}_3)\text{Cp}$  and  $(\text{Cp})_2\text{Ti}(\mu\text{-S}_2)_2\text{Ti}(\text{Cp})_2$  that have been optimized with the DFT method.



**Fig. 4.** A general interaction diagram for the model  $\text{Cp}(\text{PH}_3)\text{Ru}(\mu\text{-S}_2)_2\text{Ru}(\text{PH}_3)\text{Cp}$  of compound **9**.

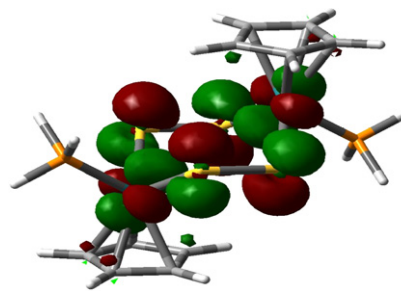


**Fig. 5.** A view of the LUMO obtained from the corresponding DFT wavefunctions computed for the  $\text{Cp}(\text{PH}_3)\text{Ru}(\mu\text{-S}_2)_2\text{Ru}(\text{PH}_3)\text{Cp}$  model of complex **6** (isovalue 0.04).

tually, the smaller energy gap determines a much greater population of  $S_4$  ( $\sigma^*-\sigma^*$ )<sub>y</sub> in **8** than in **4** (47% vs. 9%), the result confirming that the  $\text{Co}_2$  system maintains uncoupled the disulfide ligands and the presence of oxidized  $d^6$  metal atoms. However, similar to the TD complex **5**, a residual coupling cannot be excluded also in this case and, perhaps significantly, the separation between the  $S_2$  bridges is in **8** about 0.4 Å smaller than in **9–12**.

For the  $\text{CpLM}$  fragments in **9–11**, potentially *isolobal* with both  $L_4M$  and  $L_2M$  ones, the metals have a hole in their  $t_{2g}$  sets. Thus, an additional problem concerns the quenched magnetism of two  $d^5$  ions in the absence of a direct M–M bond, which could be presumed to exist between two 17-electron metal fragments. However, the M–M separation is large as it is that between the  $S_2^{2-}$  units (see Table 1). As shown by the interaction diagram for the  $\text{Cp}(\text{PH}_3)\text{Ru}(\mu\text{-S}_2)_2\text{Ru}(\text{PH}_3)\text{Cp}$  model of **9** in Fig. 4 [11], ( $\sigma^*-\sigma^*$ )<sub>y</sub> finally lies lower than  $d_{\pi}^*$  in this case, thus undoubtedly supporting donation toward the metals. This is validated by the population computed for ( $\sigma^*-\sigma^*$ )<sub>y</sub>, which is as much as 79%. Fig. 4 also shows that the four dative interactions from the two  $S_2^{2-}$  units involve all the combinations of the  $p_y$  orbitals (Fig. 1b). Additionally, the ( $\pi_z^*+\pi_z^*$ ) combination of  $p_z$  orbitals donates its electrons into the vacant  $t_{2g}$  combination  $(x^2-y^2)^*$ . In view of the five different Ru–S interactions, partial multiple M–S bonding character must be assumed. This justifies also the stabilization of the 34 framework electrons in the absence of a direct M–M bond.

These arguments are based on EHMO calculations performed with the package CACAO [20] but are fully consistent with the DFT wavefunctions, as shown by a drawing of the LUMO of **9** in Fig. 5. This is confirmed to be the antibonding level between the  $(x^2-y^2)^*$  metal FMO and the  $S_4$   $\pi_z^*+\pi_z^*$  one, as shown by the (red) lateral lobes of the  $x^2-y^2$  orbital facing the (green) lobes of the sulfur orbitals.

The electronic picture for the  $\text{Mn}_2$  species **11** is also very similar. In this case, the computed population of the  $S_4$  ( $\sigma^*-\sigma^*$ )<sub>y</sub> level is lower than in **9** (65% vs. 79%). Correspondingly, the separation between the two  $S_2^{2-}$  units is about 0.05 Å smaller, perhaps consistent with a minimum residual coupling.

The model  $\text{Cp}_2\text{Ti}(\mu\text{-S}_2)_2\text{TiCp}_2$ , **12** with  $C_{2h}$  symmetry [14], has also been optimized as a minimum at the DFT level. In view of the large separation between the  $S_2^{2-}$  bridges (3.51 Å), we assign the metal oxidation as +4 ( $d^0-d^0$  configuration). Thus, a formal 18 electron configuration (12 electrons are from the Cp ligands) is reached by each metal only if the two disulfides are able to donate together a total of six electron pairs. The interaction diagram in Fig. 6 suggests that this can be the case.

The frontier levels of each  $\text{Cp}_2$  Ti fragment are well known; since the interaction with the two Cp units involve as many as six atomic orbitals of the metal, there remain only three lower empty hybrids [18]. The combinations of the latter appear at the left side of the Fig. 6.

Only the  $1a_u$  and  $1b_g$  FMOs have a local  $d_{\pi}$  symmetry. In actuality, the six in-phase and out-of-phase combinations of the metal

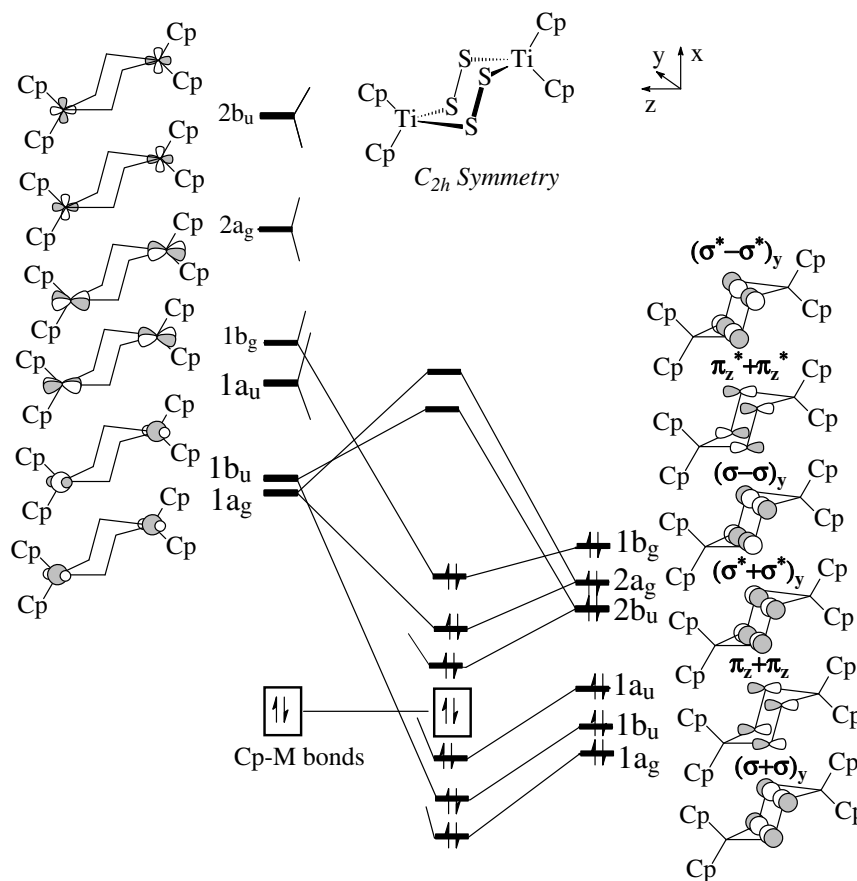


Fig. 6. Interaction diagram for the complex  $\text{Cp}_2\text{Ti}(\mu\text{-S}_2)_2\text{Ti}(\text{Cp})_2$ , **9**.

levels receive six electron pairs from the two  $\text{S}_2^{2-}$  units, which use all of their populated combinations of  $p_y$  orbitals and two  $p_z$  ones (refer to Fig. 1). Interestingly, the critical  $(\sigma^*-\sigma^*)_y$  level reaches a population of 82%, the highest value of all the compounds we have surveyed. This indicates clearly that **12** is best described as having two uncoupled disulfide anions, *i.e.*, one extreme of the  $\text{S}_4^{2-}/2\text{S}_2^{2-}$  dichotomy.

### 3. Conclusions

The MO analysis in this paper is an extension of our previous investigation [1] that led us to formulate the possible stabilization of  $\text{S}_4^{2-}$  rings in some transition metal compounds. This unusual unit may result from an external two-electron oxidation or an internal redox equilibrium that prevents the coordinated metal atoms from reaching high and unfavorable oxidation states. The present study confirms the validity of the general model based on the continuity of the  $2\text{S}_2^{2-}/\text{S}_4^{2-}$  dichotomy, according to which the donor capabilities of the bridges adapt to the electronic requirements of the metals. Thus in the triple-decker species, the  $\text{S}_4$  bridge donates up to seven electron pairs to the two iron atoms in **3**, but essentially eight pairs to the rhenium atoms in **5**. In chair-like  $\text{MS}_4\text{M}$  cores, highly deficient metals, such as Ti(IV), receive as many as six electron pairs from two parallel disulfide bridges, but the number of donor interactions is reduced to five and four in systems with  $d^5-d^5$  (**9–11**) and  $d^6-d^6$  (**8**) configurations, respectively. As occurs in **3**, the donor capabilities are reduced when the two disulfide couple together but also when the metals are electron-rich. This occurs in presence of electron-rich and electronegative metals such as copper. The latter prefers the Cu(II) versus the

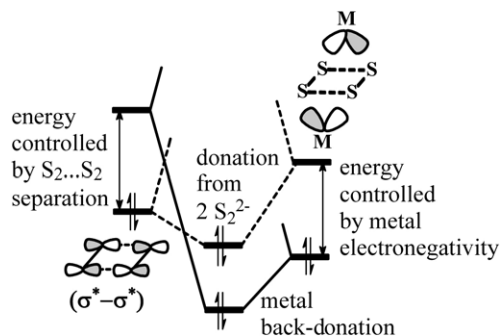


Fig. 7. Schematic diagram illustrating the direction of the electron interactions between two metal fragments and a  $\text{S}_4$  bridging unit.

Cu(III) oxidation state, hence the  $d^9-d^9$  configuration is more consistent with only three effective donations from the sulfur bridges.

In summary, a metal-ligand inner redox process can favor the stabilization of the  $\text{S}_4^{2-}$  ring. Fig. 7 schematically illustrates the parameters which seem to control the  $2\text{S}_2^{2-}/\text{S}_4^{2-}$  dichotomy.

On the right side, the appropriate combination of metal  $d_\pi$  hybrids can span a range of energies which depends on the electronegativity of the metals. On the left side, the energy of the most critical  $(\sigma^*-\sigma^*)_y$  combination also spans a significant range of energies depending on the physical separations between the two  $\text{S}_2$  units. These factors discriminate, case by case, whether the interaction is donation or back-donation from or to the bridges, respectively. In the latter case, the dichotomy is definitely shifted toward the  $\text{S}_4^{2-}$  ring. The metals have a major role in controlling

the effect but also the peculiar diffuseness and position on the electronegativity scale of the sulfur orbitals determine the remarkable flexibility of the latter to act as donors or acceptors of electrons. This is proved by the wide range of different behaviors highlighted in this paper.

#### 4. Computational details

Structural optimizations were carried out at the hybrid density functional theory (DFT) using the GAUSSIAN 03 suite of programs [21]. We built the models simplifying the ancillary ligands of the complexes. For instance, the methyl and isopropyl substituents of Cp<sup>+</sup>, Cp' and Cp'' ligands were replaced by H atoms (see Table 1). Also in **9**, the PH<sub>3</sub> ligand was used instead of triphenylphosphine.

The method used was the Becke's three-parameter hybrid exchange-correlation functional [22] containing the nonlocal gradient correction of Lee, Yang and Parr (B3LYP) [23]. The nature of the optimized structures were confirmed by calculations of the frequencies. The Stuttgart/Dresden effective core potential was used for metals [24]. The basis set used for the remaining atomic species was the 6-31G(d,p) [25]. The qualitative MO interpretation has been developed with the help of the EHMO-based CACAO package [20].

#### Acknowledgments

With great pleasure and pride C.M. dedicates this work to his old buddy and schoolmate Dante. The group in Florence kindly acknowledges CINECA for the computing time provided under the agreement with CNR. The work was carried out under the Project n. 7 of the "Dipartimento di Progettazione Molecolare" of CNR. Research at Cornell was supported by the NSF Grant CHE-0613306.

#### Appendix A. Supplementary material

Coordinates of the optimized models **8**, **9**, **11**, and **12**. Supplementary data associated with this article can be found, in the online version, at doi:10.1016/j.ica.2008.03.060.

#### References

- [1] C. Mealli, A. Ienco, A. Poduska, R. Hoffmann, *Angew. Chem., Int. Ed.* 47 (2008) 2864.
- [2] T. Nishioka, H. Kitayama, B.K. Breedlove, K. Shiomi, I. Kinoshita, K. Isobe, *Inorg. Chem.* 43 (2004) 5688.
- [3] K. Isobe, Y. Ozawa, A. Vazquez de Miguel, T.W. Zhu, K.M. Zhao, T. Nishioka, T. Ogura, T. Kitagawa, *Angew. Chem., Int. Ed.* 33 (1994) 1882.
- [4] C. Mealli, A. Ienco, A. Poduska, R. Hoffmann, in preparation.
- [5] H. Brunner, A. Merz, J. Pfauntsch, O. Serhadli, J. Wachter, M.L. Ziegler, *Inorg. Chem.* 27 (1988) 2055.
- [6] H. Ogino, H. Tobita, S. Inomata, M. Shimoi, *Chem. Commun.* (1988) 586.
- [7] J.T. York, E.C. Brown, W.B. Tolman, *Angew. Chem., Int. Ed.* 44 (2005) 7745.
- [8] R. Sarangi, J.T. York, M.E. Helton, K. Fujisawa, K.D. Karlin, W.B. Tolman, K.O. Hodgson, B. Hedman, E.I. Solomon, *J. Am. Chem. Soc.* 130 (2008) 676.
- [9] W. Tremel, R. Hoffmann, E.D. Jemmis, *Inorg. Chem.* 28 (1989) 1213.
- [10] R.J. Pleus, W. Saak, S. Pohl, *Z. Anorg. Allg. Chem.* 627 (2001) 250.
- [11] J. Amarasekera, T.B. Rauchfuss, A.L. Rheingold, *Inorg. Chem.* 26 (1987) 2017.
- [12] P.M. Treichel, R.A. Crane, K.J. Haller, *Polyhedron* 9 (1990) 1893.
- [13] A.A. Pasynskii, V.N. Grigor'ev, A.I. Blokhin, I.Yu.V. Torubaev, K.A. Lyssenko, V.V. Minin, *Russ. J. Inorg. Chem.* 50 (2005) 1450.
- [14] D.M. Giolando, T.B. Rauchfuss, A.L. Rheingold, A.R. Wilson, *Organometallics* 6 (1987) 667.
- [15] H. Brunner, J. Pfauntsch, J. Wachter, B. Nuber, M.L. Ziegler, *J. Organomet. Chem.* 359 (1989) 179.
- [16] M.R. Du Bois, B.R. Jagirdar, S. Dietz, B.C. Noll, *Organometallics* 16 (1997) 294.
- [17] H. Brunner, W. Meier, J. Wachter, E. Guggolz, T. Zahn, M.L. Ziegler, *Organometallics* 1 (1982) 1107.
- [18] T.A. Albright, J.K. Burdett, M.H. Whangbo, *Orbital Interactions in Chemistry*, Wiley, New York, 1985.
- [19] R. Hoffmann, *Angew. Chem., Int. Ed.* 21 (1982) 711.
- [20] (a) C. Mealli, D.M. Proserpio, *J. Chem. Educ.* 67 (1990) 399;  
(b) C. Mealli, A. Ienco, D.M. Proserpio, *Book of Abstracts of the XXXIII ICCS*, ICCS, Florence, Italy, 1998, p. 510.
- [21] M.J. Frisch, G.W. Trucks, H.B. Schlegel, G.E. Scuseria, M.A. Robb, J.R. Cheeseman, J.A. Montgomery Jr., T. Vreven, K.N. Kudin, J.C. Burant, J.M. Millam, S.S. Iyengar, J. Tomasi, V. Barone, B. Mennucci, M. Cossi, G. Scalmani, N. Rega, G.A. Petersson, H. Nakatsuji, M. Hada, M. Ehara, K. Toyota, R. Fukuda, J. Hasegawa, M. Ishida, T. Nakajima, Y. Honda, O. Kitao, H. Nakai, M. Klene, X. Li, J.E. Knox, H.P. Hratchian, J.B. Cross, C. Adamo, J. Jaramillo, R. Gomperts, R.E. Stratmann, O. Yazyev, A.J. Austin, R. Cammi, C. Pomelli, J.W. Ochterski, P.Y. Ayala, K. Morokuma, G.A. Voth, P. Salvador, J.J. Dannenberg, V.G. Zakrzewski, S. Dapprich, A.D. Daniels, M.C. Strain, O. Farkas, D.K. Malick, A.D. Rabuck, K. Raghavachari, J.B. Foresman, J.V. Ortiz, Q. Cui, A.G. Baboul, S. Clifford, J. Cioslowski, B.B. Stefanov, G. Liu, A. Liashenko, P. Piskorz, I. Komaromi, R.L. Martin, D.J. Fox, T. Keith, M.A. Al-Laham, C.Y. Peng, A. Nanayakkara, M. Challacombe, P.M.W. Gill, B. Johnson, W. Chen, M.W. Wong, C. Gonzalez, J.A. Pople, *GAUSSIAN 03*, Revision C.02, Gaussian, Inc., Wallingford, CT, 2004.
- [22] A.D. Becke, *J. Chem. Phys.* 98 (1993) 5648.
- [23] C. Lee, W. Yang, R.G. Parr, *Phys. Rev. B* 37 (1998) 785.
- [24] M. Dolg, H. Stoll, H. Preuss, R.M. Pitzer, *J. Phys. Chem.* 97 (1993) 5852.
- [25] P.C. Hariharan, J.A. Pople, *Theor. Chim. Acta* 28 (1973) 213.